https://doi.org/10.3311/PPch.38458

Periodica Polytechnica Chemical Engineering

Rheological Behavior and Improved Swelling of Porous Semi-IPN Hydrogels Based on Poly(isopropylacrylamide-co-itaconic Acid)/Sodium Alginate – *In Vitro* Theophylline Release Analysis

Manel Balamane[1], Djamel Aliouche[1*]

[1] Fibrous Polymer Processing and Shaping Laboratory, Faculty of Technology, M'Hamed Bougara University, Avenue de l'Indépendance, 35000 Boumerdes, Algeria
[*] Corresponding author, e-mail: aliouche.djamel@univ-boumerdes.dz

Received: 01 October 2024, Accepted: 13 January 2025, Published online: 29 January 2025

Abstract

A series of semi-interpenetrating networks (semi-IPN) hydrogels composed of temperature sensitive poly(N-isopropylacrylamide) (PNIPAAm) and pH sensitive itaconic acid (IA) and sodium alginate (SA) were prepared by radical copolymerization/crosslinking reaction. The structures, morphology, thermal, rheological and swelling behaviors of the hydrogels were studied. The evidence for successful synthesis was confirmed by infrared spectroscopy. In thermal analysis, all prepared semi-IPN samples showed a clear endotherm corresponding to a volume phase transition temperature. Morphological aspects of the samples displayed highly porous structure and expanded network depending on alginate content. Rheological analysis showed that all measured viscoelastic properties were influenced by gel composition and temperature; a sharp transition to higher values of the storage modulus *G'* was observed above the transition temperature. The swelling behavior revealed the high sensitivity of samples for temperature and pH: higher swelling was observed in simulated intestinal fluid (SIF) than in gastric one (SGF). Moreover, the swelling drops radically as the temperature rises up to 37 °C. In both fluids at 20 °C and 37 °C, the swelling is diffusion-controlled mechanism with a Fickian transport. From *in vitro* degradation study, the hydrogels were degradable in pancreatin-containing SIF solution at 37 °C and samples with higher alginate ratio showed high degradation rate. The high cumulative release of theophylline observed in SIF provides a significant improvement for drug delivery from these hydrogels to intestinal regions; the release profile displays close fitting to Korsmeyer-Peppas model with Fickian transport.

Keywords

semi-IPN hydrogel, swelling, diffusion, *in vitro* degradation, theophylline release

1 Introduction

In recent years, advances in bio active materials science have led to the development of intelligent biomaterials that react dynamically in response to the surrounding biological environment. One of the most important applications for these biomaterials is in the draw up of drug delivery systems [1–4]. These biomaterials must be built to load and release pharmaceutical drugs in a controlled and targeted means. The faculty to control drug-loading and release rates is an essential concept that supports the design and development of the drug delivery systems [5]. Thanks to their ability to fine-tune their chemical composition and physical characteristics, hydrogel polymers provide an ideal environment for drug release (DR) responses. Thus, stimuli-responsive hydrogels, especially those exhibiting multiple responses to temperature and pH changes in the gastrointestinal (GI) tract, have been developed to achieve multiple intelligent responses [6, 7]. By combining a temperature sensitive polymer usually poly(N-isopropylacrylamide) (PNIPAAm) with a pH-sensitive one in different architectures, dual-responsive materials can be obtained. Among the thermosensitive polymers, PNIPAAm is most promising because it exhibits a well-defined lower critical solution temperature (LCST) in water around 31–34 °C which is close to the body temperature. PNIPAAm hydrogels swell below LCST, and they collapse when heated above the LCST [8, 9]. However, some defects such as low biodegradability and poor mechanical strength hinder their practical applications [10]. To improve the performance of PNIPAAm, the inclusion of some other polymers inside the hydrogel matrix to make interpenetrating polymeric network system is a useful way to adjust their

Cite this article as: Balamane, M., Aliouche, D. "Rheological Behavior and Improved Swelling of Porous Semi-IPN Hydrogels Based on Poly(isopropylacrylamide-co-itaconic Acid)/Sodium Alginate – *In Vitro* Theophylline Release Analysis", Periodica Polytechnica Chemical Engineering, 2025. https://doi.org/10.3311/PPch.38458

functionalities. Mechanical characteristics, swelling/deswelling behavior, and drug loading (DL)/release pattern can be efficiently controlled [11, 12]. The two effects of temperature and pH can be combined in one single material by copolymerizing diprotic acid groups containing monomers into a thermosensitive polymer [13, 14]. In a different way, thermosensitive polymer has been associated with polysaccharides where the natural parts must ensure biodegradability, biocompatibility, and non-toxicity of the resulting biopolymer [15–17]. Oral DR requires a physiological temperature of 37 °C and specific pH in gastric or intestinal fluids; so, the pH sensitivity of DR matrix should be the key factor. Consequently, the release in these regions of the GI tract must be significantly improved. Under these conditions, various temperature- and/or pH-sensitive hydrogel configurations have been considered for this confined release [18]. The main objective of this work has been to prepare a class of hydrogels, easily degradable, highly sensitive to temperature and pH, and having good performance for drug delivery. For this purpose, semi-IPN hydrogels, based on copolymers of PNIPAAm and itaconic acid (IA) associated with sodium alginate (SA) units, have been synthesized by a free radical copolymerization/crosslinking reaction. In the synthesis, the crosslinking degree and concentration of IA monomer were kept constant for all samples. Structure and thermal properties of the gels so prepared were analyzed through Fourier transform infrared spectroscopy (FT-IR), scanning electron microscopy (SEM) and thermal analysis (DSC). Rheological behavior through the evolution of storage modulus G' of the hydrogels was examined in both frequency sweeps and ramps temperature. Subsequently, the dual-responsive character of hydrogels has been highlighted using swelling measurements in simulated gastric and intestinal fluids (SGF and SIF). Ultimately, *in vitro* samples degradation and theophylline release kinetics were evaluated to explore perspectives of these hydrogels for DR objective.

2 Experimental

2.1 Materials

N-isopropyl acrylamide (NIPAAm) and IA were provided by Sigma-Aldrich Chemie (Germany); NIPAAm was recrystallized from benzene/n-hexane (25/75) before use. SA, ammonium persulfate (APS) as initiator, N, N'-methylenebisacrylamide (MBAAm) crosslinker and N, N, N', N'-tetramethyl ethylenediamine (TEMED) accelerator, were all supplied by Sigma-Aldrich and used as received. Hydrochloric acid, potassium dihydrogen phosphate, potassium chloride and sodium hydroxide all of analytical grade from Panreac (Spain), used for the preparation of simulated body fluids. Theophylline (TPH), MW = 180.2, solubility in water = 8.0 mg mL^{-1} at 25 °C, melting temperature = 273 °C, pK_a = 8.81, was provided by Sigma-Aldrich and used as target for release studies. Deionized water was used for synthesis, swelling studies and for preparation of simulated fluids.

2.2 Preparation of the hydrogel samples

Some authors have prepared hydrogels of PNIPAAm/SA, stable at the physiological temperature, using APS as initiator and MBAAm crosslinker [19–22]. In this work, synthesis of PNIPAAm-co-IA/SA hydrogels was performed according to the procedure of Dumitriu et al. [23], through a free radical copolymerization and covalent crosslinking coupled reaction. In the procedure, NIPAAm was used as a base monomer, the comonomers were IA carrying diprotic acid groups and SA. The reaction was conducted under nitrogen in test tubes placed in ice bath for 24 h. Aqueous solution of NIPAAm and IA monomers, including APS was mixed with SA aqueous solution. The mass ratio of NIPAAm/IA monomers in the initial mixture was 95:5; while concentrations of SA were 5.0 wt%, 10.0 wt% and 20.0 wt% with respect to NIPAAm. MBAAm was added to the mixture, and then followed by TEMED. The amount of MBAAm was kept the same for all compositions (2.0 wt% with respect to NIPAAm). Subsequently, the final mixture was vigorously stirred and left steady to remove trapped air bubbles. After completion of the reaction and gel formation being observed, the crosslinked polymers (long cylindrical shape) are removed from tubes, cut into disks, dried to constant mass and then subjected to extraction with water. The gel samples were immersed in deionized water at room temperature for a week; the water was refreshed every several hours in order to allow the unreacted chemicals to leach out. Finally, extracted gels were dried in a vacuum oven at 30 °C to constant mass. The percentage gelation or gel fraction (GF) was calculated as

$$\mathrm{GF}(\%) = \frac{w_a}{w_b} \times 100 \,. \tag{1}$$

Where w_a and w_b are the mass of dry gels after and before extraction, respectively. Table 1 displays the formulations and their GF (%) used in this work.

Table 1 Synthesis details of hydrogels

Sample code	NIPAAm (mMole)	IA (mM)	SA (mM)	APS (mM)	MBAAm (mM)	TEMED (µL)	H_2O (mL)	GF (%)
I5S5	13.80	0.60	0.39	0.14	0.20	120	19.5	98.82
I5S10	13.80	0.60	0.79	0.14	0.20	120	19.5	98.30
I5S20	13.80	0.60	1.58	0.14	0.20	120	19.5	96.65

2.3 Characterization

2.3.1 Fourier transforms infrared spectroscopy

The dried hydrogels were directly analyzed using a ThermoScientific Nicolet IS 10 Model Spectrophotometer equipped with ATR Smart iTR module. The analysis was carried out with 40 scans and 2 cm^{-1} of resolution, in the range of 4000–600 cm^{-1}.

2.3.2 Thermal analysis

In DSC experiment, the hydrogel discs were first allowed to swell in deionized water at room temperature for at least 24 h to reach equilibrium. DSC analysis was carried out using TA instruments Q100 modulated DSC apparatus. Heat Flow (mW) values of the swollen hydrogels were performed from 25 to 45 °C at a heating rate of 5 °C min^{-1} under nitrogen flow (50 mL min^{-1}); the DSC curve was recorded simultaneously as a function of temperature.

2.3.3 Scanning electron microscope analysis

The equilibrium-swollen hydrogels were freeze-dried under vacuum at −40 °C for at least 24 h until all water had sublimed. Prior to analysis, the lyophilized hydrogels were fractured and coated with a thin layer of gold to prevent charging effects. The surface samples morphology was investigated using scanning electron microscope (JSM-6360LV JEOL, Japan) at various magnifications.

2.4 Rheological analysis

The viscoelastic properties of hydrogels were studied using MCR 302 (Anton Paar) rheometer equipped with parallel plate geometry (25 mm diameter and gap of 1.5 mm) and a Peltier system for accurate control of temperature. A solvent trap was used to minimize water evaporation. Prior to measurements, hydrogel discs were swollen for at least 24 h in deionized water until equilibrium. First, the linear viscoelastic region (LVE, defined as the region in which the storage and the loss modules are independent of the stress amplitude) was determined with the stress sweeps tests (0.1–100 Pa) at a constant frequency of 5.0 rad s^{-1}. Oscillatory shear tests were then performed in both frequency and temperature gradient modes:

- The frequency sweeps test was carried out on samples over a frequency range from 0.1 to 100 rad s^{-1}, at a fixed temperature and oscillation stress of 5 Pa (in the LVE limits); a normal force of 1 N was applied to the sample.
- Temperature ramps experiments were performed on samples from 23 °C (ambiant) to 50 °C, with a heating rate of 2 °C min^{-1}, under 5 Pa oscillation stress and constant frequency of 1 rad s^{-1} (normal force was set to 1 N).

2.5 Swelling behavior

Water uptake was measured at 20 °C and 37 °C in media of the USP (HCl) (pH = 1.2) and USP (phosphate) (pH = 7.4) buffers solutions used for the desired simulated gastric and intestinal fluids. For the procedure, dried pre-weighed hydrogels were immersed into vials (100 mL) filled with buffer solution and removed at regular time-intervals, wiped superficially with filter paper to extract surface-bound solution, weighed and then dipped in the same vials, at the same time fresh solution was added to keep the solution volume constant. In order to reach the swelling equilibrium degree, the gels were left in water for 24 h. All the experiments were carried out in triplicate and the average values have been reported in the data. The swelling ratio (SR) was calculated as

$$\mathrm{SR}(\%) = \frac{w_t - w_0}{w_0} \times 100\,, \tag{2}$$

where w_0 and w_t are the mass of dry gel and swollen gel at time t, respectively.

2.6 *In vitro* enzymatic degradation

For drug delivery, the matrix carrier must be degradable at the conditions of body fluids, the hydrogels degradation was studied on basis of mass loss (WL). *In vitro* experiments were conducted in SIF (pH = 7.4), with pancreatin (2 mg mL^{-1}) for 25 days. Dried pre-weighed samples were immersed in vessels containing 50 mL enzymatic SIF solution. The mixtures are then incubated in absence of light at 37 °C under constant stirring. At predetermined time

intervals, the samples are removed, thoroughly washed with SIF solution, and blotted with filter paper to remove surface solution and dried at 40 °C to constant mass. The degree of degradation is estimated by WL as

$$\mathrm{WL}(\%) = \frac{w_t}{w_0} \times 100\,, \tag{3}$$

where w_0 is the mass of dried gel before immersion and w_t is the mass of dried gel after degradation at predetermined days.

2.7 DL and encapsulation efficiency

TPH was used as model drug. TPH was loaded into hydrogels by swelling equilibrium method: dried hydrogels discs (1 mm thick, 10 mm diameter) were immersed in TPH solution (1.25 mg mL^{-1}) at 25 °C in absence of light, and then incubated for 72 h to ensure equilibrium uptake of TPH. After that time, wet TPH-loaded hydrogels were carefully taken out from the solution, washed with the same solution to remove free adhered TPH from the sample surface and at least, placed first for drying overnight at ambient temperature in dark conditions, followed by drying in a vacuum oven at 30 °C for 24 h. TPH concentration in the supernatant solution was measured using ThermoScientific Evolution 201 UV-Vis spectrophotometer at wavelength 272 nm. Amount of TPH loaded was then determined by difference in concentration of the solution before and after immersing the hydrogel samples. The experiments were carried out in triplicate and average values were taken. DL and entrapment efficiency (EE) of the samples were determined as

$$\mathrm{DL}\left(\mathrm{mg/g\ \ hydrogel}\right) = \frac{w_d - w_i}{w_i} \tag{4}$$

$$\mathrm{EE}(\%) = \frac{w_d - w_i}{w_0} \times 100\,. \tag{5}$$

Where w_i is the mass of dry hydrogel before immersing, w_d is the mass of the drug loaded dry hydrogel sample and w_0 the initial amount of TPH in solution.

2.8 *In vitro* theophylline release studies

The TPH release from hydrogels was evaluated simultaneously in both simulated fluids of SIF (pH 7.4) and SGF (pH 1.2) at 37 ± 0.5 °C and 0.1 mol/L ionic strength, with stirring speed of 50 rpm. A specific amount of TPH loaded dry hydrogel was immersed in buffer solutions of SGF or SIF respectively. At several time intervals, 5 mL of the solution containing released drug was removed and at the same time 5 mL, fresh solution was added to keep the solution volume constant. The amount of TPH released was measured and the absorbance of solution was recorded at regular time intervals at wavelength 272 nm. All release experiments were carried out in triplicates and the average values were used in the data. The DR was determined as

$$\mathrm{DR}(\%) = \frac{w_{\mathrm{drug}} - w_{\mathrm{release}}}{w_{\mathrm{release}}} \times 100\,, \tag{6}$$

where w_{drug} is the total mass of loaded TPH in the hydrogel, w_{release} is the amount of TPH released after regular time interval.

3 Results and discussion

PNIPAAm-co-IA/SA systems are prepared based on covalent crosslinking between SA and PNIPAAm-co-IA copolymers. Alginate is bonded to copolymer chains through crosslinking with MBAAm. Moreover, additional crosslinking can also take place with APS as shown in [23]. Mass ratios of NIPAAm, IA and SA in the feed with gel fraction are summarized in Table 1. From the GF (%) results, it can be noticed that the increase in alginate content within the semi-IPN samples reduces the gel fraction but at the same time improves the expanded porous structure of the hydrogels, as observed by SEM.

3.1 FT-IR analysis

Fig. 1 shows the infrared spectra of SA, PNIPAAm homopolymer and semi-IPNs I5S10 and I5S20.

The characteristic absorptions of alginate (curve SA

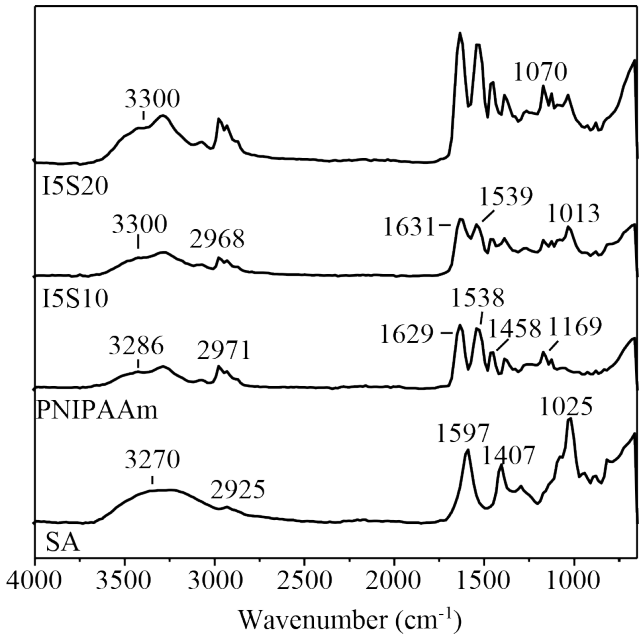

Fig. 1 FT-IR spectra of SA, PNIPAAm and PNIPAAm-co-IA/SA hydrogels

in Fig. 1) are as follow respectively: the broadband at 3270 cm^{-1} for stretching vibration of hydroxylgroups (νOH); peak of aliphatic C-H at 2925 cm^{-1}; peaks at 1597 and 1407 cm^{-1} for the asymmetric and symmetric -COO^- corresponding to vibration νC-O of carboxylic groups; and peak at 1025 cm^{-1} attributed to the C-O stretching of C-O-C group.

The PNIPAAm spectrum shows a double peak around 3286 cm^{-1} corresponding to the amine stretching vibration N-H; two characteristic bands of amide I (νCO) and amide II (νCO-NH) were detected at 1629 and 1538 cm^{-1} respectively. Peaks at 1458 and around 1367 cm^{-1} are attributed to isopropyl group in -$OCH(CH_3)_2$.

The crosslinking is confirmed by the presence of some characteristic bands of PNIPAAm, IA and SA in both spectra of I5S10 and I5S20 semi-IPN samples. Most of these bands are shifted to higher wavenumbers, indicating interactions between components. This fact is an evidence for successful synthesis of PNIPAAm-co-IA/SA hydrogels. Broad band of -OH groups of alginate has a lower intensity and is shifted to higher wavenumbers (3400 cm^{-1}); while the strong peak at 1025 cm^{-1} (C-O stretching of C-O-C) has a significantly lower intensity and it almost disappears (at 1070 cm^{-1}) in I5S20 sample, probably due to the covalent interactions between the components assisted by the MBAAm. Amide I and amide II bands are overlapped with asymmetric and symmetric -COO^- of carboxylic groups of IA and SA; these peaks are shifted to higher wavenumbers (at 1631 cm^{-1} and 1539 cm^{-1}).

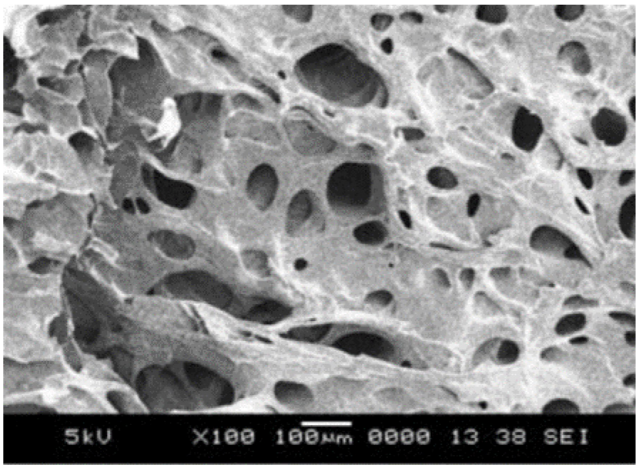

(a)

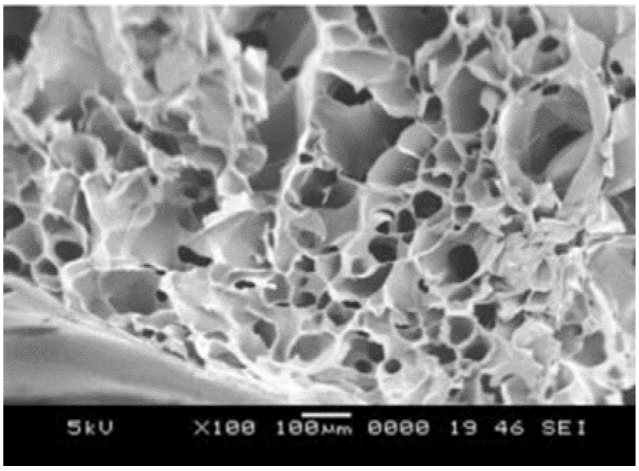

(b)

Fig. 2 SEM micrographs of the prepared semi-IPN gels: (a) I5S10, (b) I5S20

3.2 Morphological aspects of the hydrogels

Morphology of semi-IPN hydrogels has been studied by SEM analysis; Fig. 2 shows the micrographs of I5S10 (Fig. 2 (a)) and I5S20 (Fig. 2 (b)) respectively. There are distinctive differences between samples prepared with various amounts of alginate.

As seen in Fig. 2, the semi-IPN hydrogels show a relatively expanded super porous network structure with increase of alginate content [24]. The samples have many irregular interconnected pores, indicating that after the freeze-drying of the swollen hydrogels a sustained super porous network is expanded; moreover, it seems that the cavity numbers of network are improved depending on alginate content. These observations are confirmed in the Fig. 3, which shows a magnification of the internal structure of hydrogels. As seen the pore size is larger with increasing SA content in the semi-IPNs, this highly expanded network certainly resulted from the electrostatic repulsion between carboxylate anions (-COO^-) of SA and IA components after equilibrium swelling. Larger are the pores, more accessible is the internal network. In addition, some breaks in the cavity walls (as seen in Fig. 3 (b)) also promote the accessibility to water.

3.3 Thermal analysis

The collapse of the temperature-responsive hydrogels is due to the hydrophobic and hydrophilic interactions in their macromolecular chain. In PNIPAAm gels, both hydrophilic -CO-NH and hydrophobic -$CH(CH_3)_2$ groups are present. They can initiate abrupt alterations of hydrophilic/hydrophobic balance in the network at distinctive temperature so-called LCST [25]. The formation (below LCST) and rupture (above LCST) of H_2 bonds between -NH and -C=O groups and surrounding water molecules explain the temperature-sensitivity of the PNIPAAm polymer [26]. The DSC thermograms of PNIPAAm and

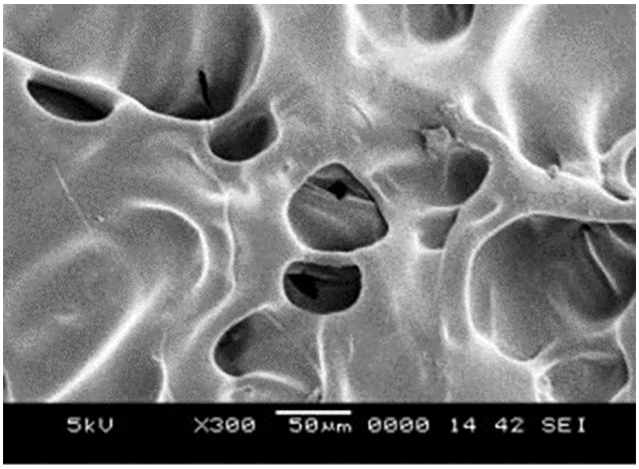

(a)

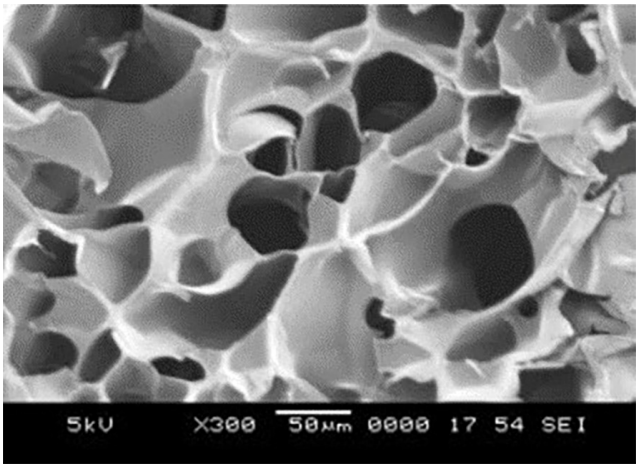

(b)

Fig. 3 Magnification of the internal structure of hydrogels: (a) I5S10, (b) I5S20

PNIPAAm-co-IA/SA gels are shown in Fig. 4. The phase transition temperature is defined as the temperature at the onset point of the DSC endotherm [27, 28]. Pure PNIPAAm exhibits a sharp endotherm at 33.5 °C, which corresponds to its LCST. For the semi-IPN samples, an endotherm can be observed at temperatures slightly lower than that of PNIPAAm, i.e., around 32 °C. In addition, we can notice that with higher SA content lower is the endotherm temperature i.e., lower is the LCST of the copolymer. This fact suggests that there is of course a crosslinking between alginate and PNIPAAm-co-IA copolymers and no significant change occurs in the balance between the hydrophobic and hydrophilic interactions in the copolymers.

3.4 Rheological analysis

After swelling at equilibrium and wiping excess water from the surface of samples, the rheological tests were performed in the LVE region. to assess first, the frequency sweeps

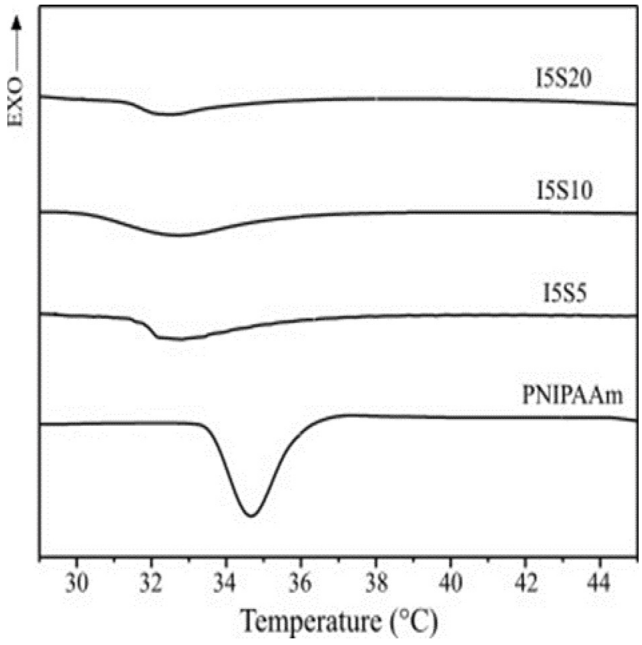

Fig. 4 DSC thermograms of PNIPAAm and semi-IPN copolymers

profiles of the gels at various temperatures. The value of storage modulus G' is associated with the hydrogel strength and stiffness; an increase in G' value suggests the higher hydrogel mechanical strength and rigidity. The following Fig. 5 shows the mechanical spectra for swollen hydrogels of PNIPAAm-co-IA/SA copolymers. From Fig. 5 it can be observed that in the whole temperature range considered, G' shows no dependence on frequency for all the samples investigated as expected the elastic behavior of samples predominates and the swollen samples exhibit mechanical rigidity. This finding suggests that the semi-IPN samples are well-crosslinked and agree with the requirements for a solid-like elastic gel [29]. A similar behavior has already been observed by Bashir et al. [30] for hydrogels based on N-succinyl chitosan grafted poly(acrylic acid). A clear decrease of G' is observed with increasing alginate content within the semi-IPNs, which seems to be due to the increased porosity of the samples.

Indeed, as seen in morphological section, higher alginate content implies a more porous network with large cavities that are more easily broken and thus weaken the polymer structure with lower mechanical strength. It is clear that the presence of PNIPAAm into semi-IPN gels is the key factor for an improved mechanical response; more PNIPAAm in the copolymers resulted in higher storage modulus values [31]. On the other hand, at the temperature near of the PNIPAAm LCST, all samples undergo a phase transition which initiates shrinkage of their internal network with drastic decrease of G'. This critical decrease

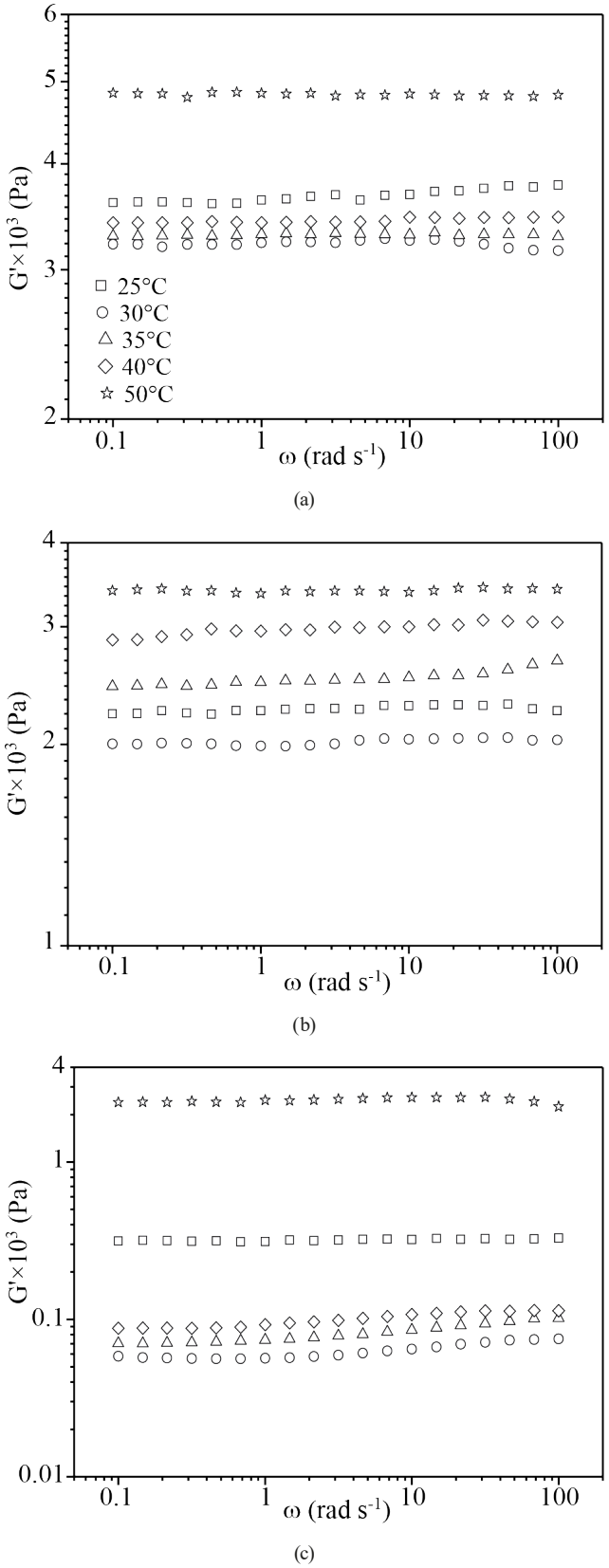

Fig. 5 Effect of temperature on storage modulus (G') for (a) I5S5; (b) I5S10 and (c) I5S20 samples

in G' should be due to the collapse of PNIPAAm chains produced by the quick changes between the hydrophilic/hydrophobic balance at the LCST. By increasing temperature higher than 35 °C a thermothickening effect is observed and G' is significantly increased for all samples. This finding is showed to be more pronounced for the I5S5 sample (with less alginate content) where the G' values were twice compared to those measured at 25 °C. With comparable results, de Moura et al. [32] suggested that at temperatures above the LCST, PNIPAAm chains shrink, and hydrogels based on alginate and PNIPAAm have a rigid structure with smaller pore size and are stronger when subjected to mechanical deformation test.

Fig. 6 shows the oscillatory temperature sweep profiles of the semi-IPN hydrogels from 24 to 50 °C.

The overall thermal behavior of the samples is comparable, that is, a clear transition is observed above the PNIPAAm LCST followed with increase in the storage modulus G' from low to higher values as temperature increases: under these conditions, the strengthening of the gels becomes more pronounced. As seen above, this transition can be attributed to the collapse of PNIPAAm blocks: above LCST these segments aggregate into hydrophobic domains and form intermolecular hydrophobic association with the alginate side chains [33]. The expansion of this strong gel-like structure by increasing temperature should be related to a thermothickening effect due to the PNIPAAm-co-IA copolymer parts within the semi-IPN structure. This effect is seen to be more significant for the semi-IPNs with a lower SA content. This behavior was attributed by some authors to the dehydration of polymers and destruction of physical crosslinks in the gel network, which leads to an increase in storage modulus at first step [34]. With further heating above 45 °C, an equilibrium plateau tends to establish without any further increase.

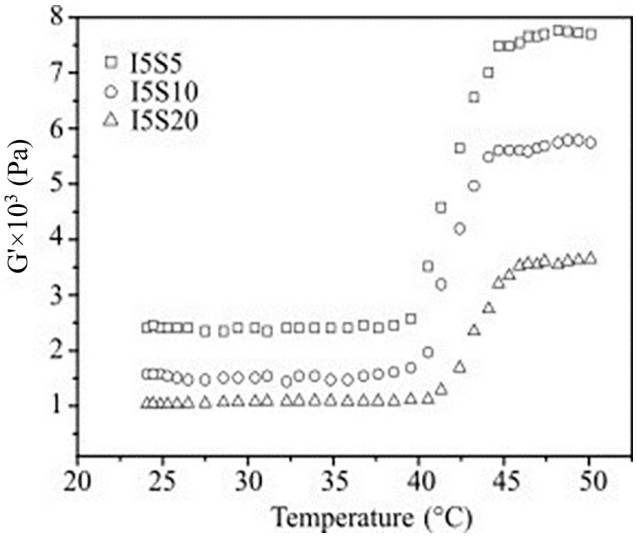

Fig. 6 Temperature ramps test for the semi-IPN gels

3.5 Swelling behavior

In drug delivery systems, the volumetric changes of carrier during swelling need to be controlled rigorously in order to initiate release of drug molecules under suitable functional conditions [35]. Here we focused on the gel performance in the physiological conditions of body fluids. In these environments, the equilibrium swelling of the gels can be suitably exploited for delivery to the GI tract where the pH changes from acidic in the stomach to basic in the intestine.

3.5.1 Swelling kinetics

The SR of hydrogels is evaluated at different time intervals and the data were fitted to the second-order rate equation [36, 37]. From the same equation the initial rate of swelling r_0 can be deduced. The fitting of swelling data was carried out and the parameter values of the second order equation are adjusted in an iterative process using χ^2. The validity of the kinetic model was evaluated in terms of regression coefficient R^2, nonlinear χ^2 and F values obtained from Anova analysis. A good fitting implies R^2 close to 1, χ^2 with low values and high values of parameter F. The data of experimental and calculated equilibrium swelling ratio (ESR) obtained from the second order kinetic equation are summarized in Tables 2 and 3 for the swelling at 20 °C and 37 °C respectively. Tables 2 and 3 display the results as a function of medium (SIF and SGF) including values of r_0, k_s and statistical parameters (R^2, χ^2, and F).

For all samples, the data show good fitting to second order equation, the effect of pH on the swelling is significant: the samples shrink in SGF and swell in SIF. For these gels, we can also note that both initial rate of swelling and ESR are function of alginate content in the copolymers: in SIF, both parameters increase with increased SA content while in the SGF the opposite is observed. From Table 3, it can be observed that the cumulative effect of temperature on the swelling is instantaneous and the drop of ESR for all samples is drastic. At physiological temperature (37 °C) the initial rate of swelling and SR of all hydrogels are decreased for 4–5 times compared to 20 °C. This can be explained by the shrinkage of PNIPAAm component around its LCST transition. In addition to the swelling kinetics, the diffusion kinetics was analyzed for both SGF and SIF media at 20 °C and 37 °C.

3.5.2 Diffusion kinetics

Diffusion of water molecules within hydrogel is a phenomenon of great consequence for its DR functions. To

Table 2 Swelling kinetics data of gels in SIF and SGF at 20 °C

Sample	ESR_{exp}/ESR_{cal} (%)	$k_s \times 10^{-6}$	r_0	R^2	$\chi^2 \times 10^{-5}$	F
			SIF 20 °C			
I5S5	4810.6/5429.2	1.41	41.56	0.994	3.10	2704.9
I5S10	4945.2/5488.7	1.62	48.80	0.995	2.20	3536.6
I5S20	5595.8/6131.9	1.58	59.41	0.997	1.12	5409.3
			SGF 20 °C			
I5S5	1302.3/1463.5	5.34	11.44	0.994	36.30	3142.5
I5S10	1231.8/1370.1	6.16	11.56	0.996	30.50	4153.0
I5S20	1217.9/1368.5	5.60	10.49	0.995	38.60	3401.1

Table 3 Swelling kinetics data of gels in SIF and SGF at 37 °C

Sample	ESR_{exp}/ESR_{cal} (%)	$k_s \times 10^{-6}$	r_0	R^2	$\chi^2 \times 10^{-4}$	F
			SIF 37 °C			
I5S5	935.3/1017.0	9.6	9.93	0.997	3.5	6232.6
I5S10	1019.2/1138.4	7.1	9.20	0.995	5.2	3612.1
I5S20	1217.9/1333.6	7.0	12.4	0.997	2.5	5127.1
			SGF 37 °C			
I5S5	283.5/326.8	19.8	2.11	0.991	120.0	2000.1
I5S10	226.5/261.1	24.5	1.67	0.991	190.0	1971.8
I5S20	197.8/227.3	28.7	1.48	0.993	210.0	2411.5

understand the water diffusion at swelling equilibrium fusion mechanism within the gel, diffusional characteristics were obtained from fractional water uptake (F), by direct nonlinear fitting of the swelling data to the model proposed by Ritger and Peppas [38], this model is based on the relative rates of penetrant diffusion and polymer chain relaxation:

$$F = \frac{w_t}{w_e} = k_D \times t^n , \quad (7)$$

where w_e (%) is the gel swelling at equilibrium, w_t (%) is the swelling at time t, the diffusion constant k_D is associated to structure of the gel and n is the diffusional exponent, it indicates the type of transport through the gel.

This equation is applicable to the initial stages of swelling (<60%) where a linear fit of the data is observed. In this power law model, the mechanism of water transport is described by two limiting cases: diffusion-controlled (Fickian with $n \leq 0.5$) and relaxation-controlled (non-Fickian with $n = 1$). The intermediate case, called anomalous diffusion, occurs when water transport is proportional to t^n (with $0.5 < n < 1$) where the rates of diffusion and polymer relaxation are comparable.

The diffusion coefficient (D) of water through cylindrical hydrogels of radius r was obtained from k_D and n as

$$D = \pi r^2 \left(\frac{k_D}{4} \right)^{\frac{1}{n}} . \quad (8)$$

Diffusion kinetics was studied for both simulated body fluids, the values of diffusion characteristics (n, D) and statistical parameters are shown in Tables 4 and 5 at 20 °C and 37 °C, respectively.

As seen, for both fluids and temperatures, all samples exhibited Fickian diffusion with n values in the range of 0.39–0.48 at 20 °C and 0.38–0.48 at 37 °C. In both fluids, most values of diffusion coefficient (D) seem to increase moderately with SA content and decrease with increasing temperature. From Tables 2–4, we can also notice that statistical parameters (R^2, χ^2 and F) confirmed the good fitting of swelling data to the power equation of diffusion for both environments.

3.6 *In vitro* enzymatic degradation

After release, the hydrogel carrier must be degraded and then, cleared from the body after use; the degradation is usually tested under internal physiological conditions of the human body. In this work, we have studied the degradation of the prepared sample for 25 days with pancreatin through *in vitro* tests in SIF at 37 °C. The results are presented in Fig. 7.

Table 4 Diffusion kinetics data of gels in SIF and SGF at 20 °C

Sample	n	k_D	$D \times 10^{-4}$ (cm^2 s^{-1})	R^2	$\chi^2 \times 10^{-3}$	F
			SIF 20 °C			
I5S5	0.45	0.050	1.18	0.965	2.50	978.4
I5S10	0.42	0.064	1.06	0.957	3.01	881.3
I5S20	0.39	0.073	0.71	0.963	2.41	1136.0
			SGF 20 °C			
I5S5	0.44	0.054	1.12	0.955	3.21	772.6
I5S10	0.42	0.061	0.96	0.954	3.22	801.4
I5S20	0.44	0.053	1.11	0.959	2.83	862.4

Table 5 Diffusion kinetics data of gels in SIF and SGF at 37 °C

Sample	n	k_D	$D \times 10^{-4}$ (cm^2 s^{-1})	R^2	$\chi^2 \times 10^{-3}$	F
			SIF 37 °C			
I5S5	0.38	0.078	0.64	0.972	1.68	1606.8
I5S10	0.44	0.055	1.20	0.966	2.33	1068.4
I5S20	0.40	0.071	0.84	0.974	1.65	1609.7
			SGF 37 °C			
I5S5	0.48	0.040	1.44	0.957	3.15	714.6
I5S10	0.48	0.041	1.44	0.963	2.65	841.4
I5S20	0.47	0.041	1.23	0.966	2.41	924.1

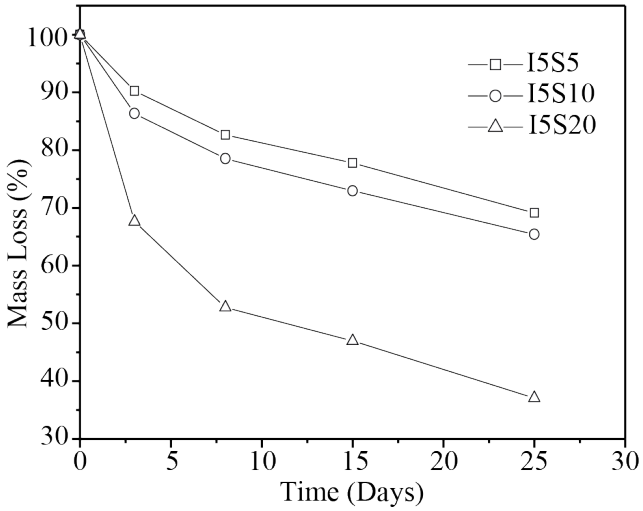

Fig. 7 Enzymatic degradation profiles of the semi-IPN hydrogels

The plotted curves suggested that the hydrogels are degradable materials and degradation started at alginate backbone as it is a natural polymer. Hence, within three days, the degradation started for all samples; after first week, the mass losses reached about 17%, 22% and 47% for the I5S5, I5S10 and I5S20 hydrogels respectively. After 25 days, the losses reach between 30 and 65% depending on the SA content. Thus, hydrogels with higher SA ratio showed high degradation rate. On the other hand, PNIPAAm as synthetic polymer has low degradation rate compared to natural polymers and therefore is more resistant to enzymatic attack: this is why the degradation is not complete. Alternatively, for all samples the presence of hydrophilic groups -OH, -NH_2 and -COOH may play a role in degradation of the hydrogels. These groups strongly interact with the solvent and weaken the internal network due to their large absorption capacity. Similar results on the degradation behavior of polysaccharide-based hydrogels can be found in the literature [39, 40].

3.7 DL and encapsulation efficiency

In order to test ability of the prepared hydrogels for DR application, TPH was used as a model drug. Physical adsorption of the TPH molecule by the hydrogels will be promoted by their complete ionization and affinity between the cationic groups of the drug and carboxyl groups of IA and alginate. The loading and entrapment efficiency of TPH drug for the various gel formulations are shown in Table 6.

As seen from Table 6, similar to SR, the loading and entrapment efficiencies of the drug are also observed to increase with increase in alginate content. Hence, due to increased swelling, the expansion of polymer network is improved and then more amount of drug is adsorbed within the hydrogels and on their surface.

Table 6 DL and encapsulation efficiency of TPH

Sample	DL (mg g^{-1})	EE (%)
I5S5	0.43	51.2
I5S10	0.51	73.6
I5S20	0.55	86.4

3.8 *In vitro* theophylline release studies

In drug delivery system the chemical structure, polymer composition and structure of the internal network strongly affect the release conditions. On the other hand, the chemical structure and molecular mass of the drug play an important role. Here, the TPH release, *in vitro*, from the prepared hydrogels was evaluated in SIF and SGF at 37 °C. The kinetic profiles of the release in both fluids are shown in Fig. 8. As for swelling, a significant increase in

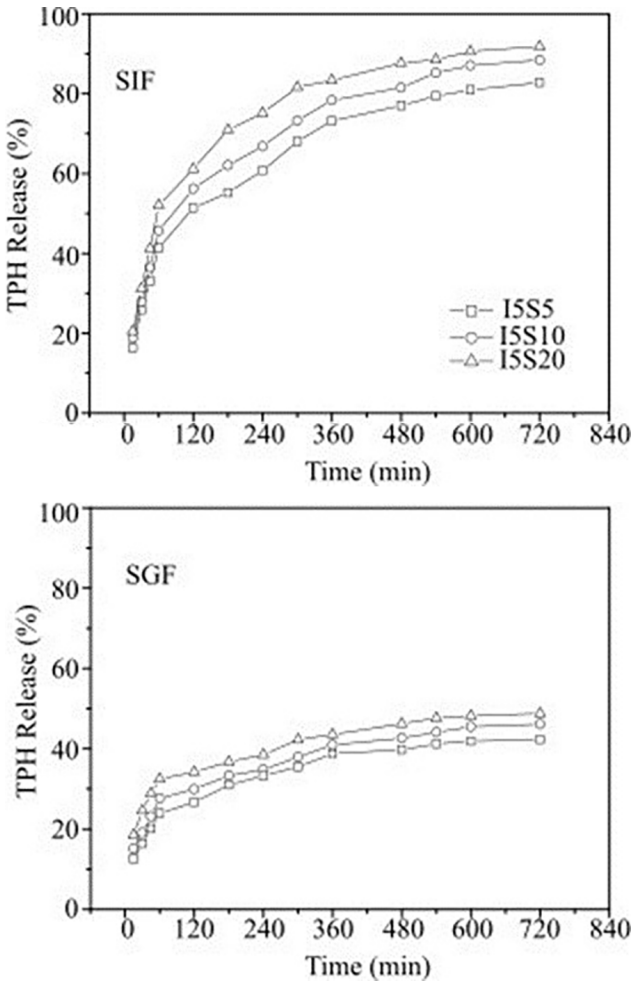

Fig. 8 Profiles of theophylline release from semi-IPN gels

TPH release rates was observed with increasing SA content in the semi-IPN hydrogels. From the Fig. 8, it was observed that for all samples the release process occurs in two stages: first, a rapid initial burst followed by a second phase with a slower release. The primary burst is initiated by the release of TPH molecules adsorbed at the surface of swollen hydrogels while the gradual release is due to diffusion from the water-filled pores and channels in the internal structure. At the physiological temperature, the cumulative release of TPH was greater in SIF than in SGF for all samples, which is consistent with the swelling test results (Table 5). This lower amount of TPH released in SGF is most likely related to the low swelling of the gels in acidic conditions due to the protonation of carboxylate ions present in copolymers; however, in SIF, the release occurs from the increasing swelling due to electrostatic repulsion through the ionization of carboxylate ions.

Consequently, in the first 3 h, the amount of TPH released in SGF reached up to 38%. At longer release time (12 h) the release rate slows down and the release amounts reached a maximum of 42%, 46% and 48% for I5S5, I5S10 and I5S20 samples respectively. In contrast, significant TPH release was observed in SIF where the total percent release could reach about 71–92% for these semi-IPNs.

Moreover, the TPH release was also highly depending on the alginate content. Thus, the release from these hydrogel samples is fast at the beginning but then it shows the behavior of a prolonged release system. In these conditions, the TPH molecule diffuses out at a faster rate; the whole release rate is controlled by the swelling rate of hydrogels. Similar release profiles were reported for theophylline release from various IPN hydrogels based on alginate and chitosan [41–43]. To find out the mechanism of TPH release process, the data were analyzed using various empirical or semi- empirical model equations that have established to be very appropriate to evaluate the first 60% of the release curve. TPH release data of the prepared samples were fitted into the following kinetic equations: Donbrow-Samuelov zero-order model [44], Higuchi model [45] and Korsmeyer-Peppas power equation [46]. A criterion for selecting the most adequate model is based on the best fit of the release data indicated by the values of the statistical parameters (values of R^2, χ^2 and F). In this way, the fitting results of the release data in both simulated fluids are shown in Table 7 for the two first models. At first sight, these models are unsuitable to explain the TPH release from the prepared gels. Although the release rates are much higher than those of Higuchi model are, the statistical parameters for zero order equation are rather low and irrelevant for illustrating the TPH release from these samples.

However, from Table 8, the TPH release data is observed to give certainly close fitting to Korsmeyer-Peppas

Table 7 Release kinetics in SIF and SGF

Model	Zero-Order			Higuchi		
Sample	$K_0 \times 10^{-2}$	R^2	χ^2/F	$K_H \times 10^{-2}$	R^2	$\chi^2 \times 10^{-2}/F$
			SIF			
I5S5	8.61	0.829	85.7/279.0	3.93	0.860	0.84/681.5
I5S10	8.98	0.814	102.9/270.8	4.00	0.827	1.01/581.0
I5S20	8.87	0.748	147.0/219.2	4.18	0.720	1.64/392.9
			SGF			
I5S5	3.92	0.826	18.2/373.5	4.17	0.678	1.61/397.4
I5S10	4.00	0.847	16.2/492.4	4.21	0.555	1.98/330.4
I5S20	3.70	0.822	16.7/583.9	4.39	0.781	3.30/216.0

Table 8 Korsmeyer-Peppas release mechanism data of gels in SIF and SGF

Sample	n	$K_{KP} \times 10^{-2}$	$D \times 10^{-6}$ (cm^2 s^{-1})	R^2	$\chi^2 \times 10^{-3}/F$
			SIF		
I5S5	0.34	10.14	40.72	0.973	1.59/1815.7
I5S10	0.33	11.13	38.88	0.970	1.75/1716.9
I5S20	0.30	13.70	26.26	0.945	3.20/1029.0
			SGF		
I5S5	0.28	15.00	16.23	0.980	1.00/3283.5
I5S10	0.26	17.19	11.14	0.983	0.76/4474.4
I5S20	0.22	23.63	5.24	0.974	0.92/4078.7

equation, which is the best fit for our results (see values of R^2, χ^2 and F). This model is useful when more than one mechanism is involved in DR: diffusion-controlled mechanism i.e., $n < 0.45$ or polymer relaxation-controlled system when $0.45 < n < 0.89$. As seen from Table 8, at same temperature (37 °C) and in both fluids, the release from all semi-IPN samples follows the same mechanism with n values in the range of 0.30–0.36 in SIF and 0.22–0.33 in SGF meaning that the release occurs through a Fickian process of controlled diffusion. Furthermore, the small values of K_{KP} in both fluids indicate the weak interaction between TPH molecule and hydrogels [47]; these values were seen to increase when the release move from SIF to SGF.

4 Conclusion

Dual responsive semi-IPN hydrogels were prepared by free radical copolymerization/crosslinking. The semi-IPN hydrogels prepared showed a super porous structure, as revealed by FTIR and observed by SEM. As shown by DSC, the hydrogels exhibit a volume phase transition at a temperature depending on the alginate content. The rheological oscillatory shear tests conducted on swollen hydrogels, confirmed that the samples behave as a strong gel. All the measured storage modulus properties are influenced by gel composition and temperature: higher alginate content implies a weaker mechanical strength. The temperature sweep test showed that around the critical temperature, all gel samples undergo a phase transition, and the dynamic modulus rises abruptly. Above the LCST a strong transition to higher values of G' occurs and the gel strengthening becomes more pronounced. The swelling behavior revealed their high temperature and pH sensitivity of the hydrogels. A higher swelling in SIF was observed as compared to SGF. In swelling kinetics, the data showed close fitting to second order rate equation and followed Fickian transport. *In vitro* degradation tests the hydrogel samples showed good degradability by pancreatin solution in SIF medium at 37 °C; and that the gels with higher SA ratio showed high degradation rate. In theophylline release studies, the semi-IPNs exhibited behavior of modulated release system where the DR is controlled by the external cumulative stimuli of temperature and pH. Release kinetics showed close fitting to Korsmeyer-Peppas model with Fickian process of controlled-diffusion. Thus, the high cumulative release in SIF provides a substantial upgrade in the drug delivery from these hydrogels. With these performances, the release profile of theophylline accomplished the oral drug delivery requirement of US pharmacopeia, which advises at least 80% of drug should be released in SIF. Therefore, after 13 h the release of 83%, 88% and 92% of the gels I5S5, I5S10 and I5S20 respectively, is also a significant advantage for their potential application in drug delivery systems.

References

[1] Trucillo, P. "Biomaterials for Drug Delivery and Human Applications", Materials, 17(2), 456, 2024. https://doi.org/10.3390/ma17020456

[2] Pires, P. C., Mascarenhas-Melo, F., Pedrosa, K., Lopes, D., Lopes, J., Macário-Soares, A., Peixoto, D., Giram, P. S., Veiga, F., Paiva-Santos, A. C. "Polymer-based Biomaterials for Pharmaceutical and Biomedical Applications: A Focus on Topical Drug Administration", European Polymer Journal, 187, 111868, 2023. https://doi.org/10.1016/j.eurpolymj.2023.111868

[3] Troy, E., Tilbury, M. A., Power, A. M., Wall, J. G. "Nature-Based Biomaterials and Their Application in Biomedicine", Polymers, 13, 3321, 2021. https://doi.org/10.3390/polym13193321

[4] Webber, M. J., Pashuck, E. T. "(Macro)molecular self-assembly for hydrogel drug delivery", Advanced Drug Delivery Reviews, 172, pp. 275–295, 2021. https://doi.org/10.1016/j.addr.2021.01.006

[5] Ferreira, N. N., Ferreira, L. M. B., Cardoso, V. M. O., Boni, F. I., Souza, A. L. R., Gremião, M. P. D. "Recent advances in smart hydrogels for biomedical applications: From self-assembly to functional approaches", European Polymer Journal, 99, pp. 117–133, 2018. https://doi.org/10.1016/j.eurpolymj.2017.12.004

[6] Ding, H., Tan, P., Fu, S., Tian, X., Zhang, H., Ma, X., Gu, Z., Luo, K. "Preparation and application of pH-responsive drug delivery systems", Journal of Controlled Release, 348, pp. 206–238, 2022. https://doi.org/10.1016/j.jconrel.2022.05.056

[7] Guragain, S., Bastakoti, B. P., Malgras, V., Nakashima, K., Yamauchi, Y. "Multi-Stimuli-Responsive Polymeric Materials", Chemistry - A European Journal, 21(38), pp. 13164–13174, 2015. https://doi.org/10.1002/chem.201501101

[8] Tang, L., Wang, L., Yang, X., Feng, Y., Li, Y., Feng, W. "Poly(*N*-isopropylacrylamide)-based smart hydrogels: Design, properties and applications", Progress in Materials Science, 115, 100702, 2021. https://doi.org/10.1016/j.pmatsci.2020.100702

[9] Xu, X., Liu, Y., Fu, W., Yao, M., Ding, Z., Xuan, J., Li, D., Wang, S., Xia, Y., Cao, M. "Poly(N-isopropylacrylamide)-based thermoresponsive composite hydrogels for biomedical applications", Polymers, 12(3), 580, 2020. https://doi.org/10.3390/polym12030580

[10] Haq, M. A., Su, Y., Wang, D. "Mechanical properties of PNIPAM based hydrogels: A review", Materials Science and Engineering: C, 70, pp. 842–855, 2017. https://doi.org/10.1016/j.msec.2016.09.081

[11] Matricardi, P., Di Meo, C., Coviello, T., Hennink, W. E., Alhaique, F. "Interpenetrating polymer networks polysaccharide hydrogels for drug delivery and tissue engineering", Advanced Drug Delivery Reviews, 65(9), pp. 1172–1187, 2013. https://doi.org/10.1016/j.addr.2013.04.002

[12] Zoratto, N., Matricardi, P. "4 - Semi-IPNs and IPN-based hydrogels", In: Polymeric Gels: Characterization, Properties and Biomedical Applications, Woodhead Publishing, 2018, pp. 91–124. ISBN 9780081021798 https://doi.org/10.1016/B978-0-08-102179-8.00004-1

[13] Fathi, M., Alami-Milani, M., Geranmayeh, M. H., Barar, J., Erfan-Niya, H., Omidi, Y. "Dual thermo-and pH-sensitive injectable hydrogels of chitosan/(poly(*N*-isopropylacrylamide-*co*-itaconic acid)) for doxorubicin delivery in breast cancer", International Journal of Biological Macromolecules, 128, pp. 957–964, 2019. https://doi.org/10.1016/j.ijbiomac.2019.01.122

[14] Rwei, S.-P., Tuan, H. N. A., Chiang, W.-Y., Way, T.-F. "Synthesis and Characterization of pH and Thermo Dual-Responsive Hydrogels with a Semi-IPN Structure Based on *N*-Isopropylacrylamide and Itaconamic Acid", Materials, 11(5), 696, 2018. https://doi.org/10.3390/ma11050696

[15] Liu, M., Zhu, J., Song, X., Wen, Y., Li, J. "Smart Hydrogel Formed by Alginate-*g*-Poly(N-isopropylacrylamide) and Chitosan through Polyelectrolyte Complexation and Its Controlled Release Properties", Gels, 8(7), 441, 2022. https://doi.org/10.3390/gels8070441

[16] Tang, Q., Qian, S., Chen, W., Song, X., Huang, J. "Preparation and characterization of temperature-responsive Ca–alginate/poly(*N*-isopropylacrylamide) hydrogel", Polymer International, 72(2), pp. 252–262, 2023. https://doi.org/10.1002/pi.6464

[17] Ansari, M. J., Rajendran, R. R., Mohanto, S., Agarwal, U., Panda, K., Dhotre, K., …, Pramanik, S. "Poly(*N*-isopropylacrylamide)-Based Hydrogels for Biomedical Applications: A Review of the State-of-the-Art", Gels, 8(7), 454, 2022. https://doi.org/10.3390/gels8070454

[18] Smagina, V., Yudaev, P., Kuskov, A., Chistyakov, E. "Polymeric Gel Systems Cytotoxicity and Drug Release as Key Features for their Effective Application in Various Fields of Addressed Pharmaceuticals Delivery", Pharmaceutics, 15(3), 830, 2023. https://doi.org/10.3390/pharmaceutics15030830

[19] Lin, X., Guan, X., Wu, Y., Zhuang, S., Wu, Y., Du, L., Zhao, J., Rong, J., Zhao, J., Tu, M. "An alginate/poly(*N*-isopropylacrylamide)-based composite hydrogel dressing with stepwise delivery of drug and growth factor for wound repair", Materials Science and Engineering: C, 115, 111123, 2020. https://doi.org/10.1016/j.msec.2020.111123

[20] Qin, Z., Zhang, R., Xu, Y., Cao, Y., Xiao, L. "A one-pot synthesis of thermosensitive PNIPAAM interpenetration polymer networks(IPN) hydrogels", JCIS Open, 1, 100002, 2021. https://doi.org/10.1016/j.jciso.2021.100002

[21] Feng, J., Dou, J., Zhang, Y., Wu, Z., Yin, D., Wu, W. "Thermosensitive Hydrogel for Encapsulation and Controlled Release of Biocontrol Agents to Prevent Peanut Aflatoxin Contamination", Polymers, 12(3), 547, 2020. https://doi.org/10.3390/polym12030547

[22] Ziminska, M., Wilson, J. J., McErlean, E., Dunne, N., McCarthy, H. O. "Synthesis and Evaluation of a Thermoresponsive Degradable Chitosan-Grafted PNIPAAm Hydrogel as a "Smart" Gene Delivery System", Materials, 13(11), 2530, 2020. https://doi.org/10.3390/ma13112530

[23] Dumitriu, R. P., Mitchell G. R., Vasile, C. "Multi-responsive hydrogels based on *N*-isopropylacrylamide and sodium alginate", Polymer International, 60(2), pp. 222–233, 2011. https://doi.org/10.1002/pi.2929

[24] Zhang, G.-Q., Zha, L.-S., Zhou, M.-H., Ma, J.-H., Liang, B.-R. "Rapid deswelling of sodium alginate/poly(*N*-isopropylacrylamide) semi-interpenetrating polymer network hydrogels in response to temperature and pH changes", Colloid and Polymer Science, 283(4), pp. 431–438, 2005. https://doi.org/10.1007/s00396-004-1172-6

[25] Kumar, A., Srivastava, A., Galaev, I. Y., Mattiasson, B. "Smart polymers: physical forms and bioengineering applications", Progress in Polymer Science, 32(10), pp. 1205–1237, 2007. https://doi.org/10.1016/j.progpolymsci.2007.05.003

[26] Li, Z., Liang, B. "Modulation of phase transition of poly(*N*-isopropylacrylamide)-based microgels for pulsatile drug release", Polymers for Advanced Technologies, 33(3), pp. 710–722, 2022. https://doi.org/10.1002/pat.5421

[27] Ren, H., Qiu, X.-P., Shi, Y., Yang, P., Winnik, F. M. "The Two Phase Transitions of Hydrophobically End-Capped Poly(*N*-isopropylacrylamide)s in Water", Macromolecules, 53(13), pp. 5105–5115, 2020. https://doi.org/10.1021/acs.macromol.0c00487

[28] Krakovský, I., Hanyková, L., Šťastná, J. "Phase transition in polymer hydrogels investigated by swelling, DSC, FTIR and NMR", Journal of Thermal Analysis and Calorimetry, 2024. https://doi.org/10.1007/s10973-024-13380-5

[29] Lejardi, A., Hernández, R., Criado, M., Santos, J. I., Etxeberria, A., Sarasua, J. R., Mijangos, C. "Novel hydrogels of chitosan and poly(vinyl alcohol)-g-glycolic acid copolymer with enhanced rheological properties", Carbohydrate Polymers, 103, pp. 267–273, 2014. https://doi.org/10.1016/j.carbpol.2013.12.040

[30] Bashir, S., Teo, Y. Y., Ramesh, S., Ramesh, K., Mushtaq, M. W. "Rheological behavior of biodegradable *N*-succinyl chitosan-*g*-poly (acrylic acid) hydrogels and their applications as drug carrier and in vitro theophylline release", International Journal of Biological Macromolecules, 117, pp. 454–466, 2018. https://doi.org/10.1016/j.ijbiomac.2018.05.182

[31] Dumitriu, R. P., Mitchell, G. R., Vasile, C. "Rheological and thermal behavior of poly(*N*-isopropylacrylamide)/alginate smart polymeric networks", Polymer International, 60(9), pp. 1398–1407, 2011. https://doi.org/10.1002/pi.3093

[32] de Moura, M. R., Guilherme, M. R., Campese, G. M., Radovanovic, E., Rubira, A. F., Muniz, E. C. "Porous alginate-Ca^{2+} hydrogels interpenetrated with PNIPAAm networks: Interrelationship between compressive stress and pore morphology", European Polymer Journal, 41(12), pp. 2845–2852, 2005. https://doi.org/10.1016/j.eurpolymj.2005.06.007

[33] Kim, Y.-W., Kim, D. Y., Sun, J.-Y. "Fracture Toughness and Blocking Force of Temperature-Sensitive PolyNIPAAm and Alginate Hybrid Gels", Gels, 8(5), 324, 2022. https://doi.org/10.3390/gels8050324

[34] Safakas, K., Saravanou, S.-F., Iatridi, Z., Tsitsilianis, C. "Thermo-Responsive Injectable Hydrogels Formed by Self-Assembly of Alginate-Based Heterograft Copolymers", Gels, 9(3), 236, 2023. https://doi.org/10.3390/gels9030236

[35] Peppas, N. A., Hilt, J. Z., Khademhosseini, A., Langer, R. "Hydrogels in biology and medicine: From molecular principles to bionanotechnology", Advanced Materials, 18(11), pp. 1345–1360, 2006. https://doi.org/10.1002/adma.200501612

[36] Yavari, N., Azizian, S. "Mixed diffusion and relaxation kinetics model for hydrogels swelling", Journal of Molecular Liquids, 363, 119861, 2022. https://doi.org/10.1016/j.molliq.2022.119861

[37] Duan, J., Huang, Y., Zong, S., Jiang, J. "Preparation and drug release properties of a thermo sensitive GA hydrogel", Polymers, 13(1), 119, 2021. https://doi.org/10.3390/polym13010119

[38] Ritger, P. L., Peppas, N. A. "A simple equation for description of solute release II. Fickian and anomalous release from swellable devices", Journal of Controlled Release, 5(1), pp. 37–42, 1987. https://doi.org/10.1016/0168-3659(87)90035-6

[39] Sobczak, M. "Enzyme-responsive hydrogels as potential drug delivery systems—State of knowledge and future prospects", International Journal of Molecular Sciences, 23(8), 4421, 2022. https://doi.org/10.3390/ijms23084421

[40] Knipe, J. M., Chen, F., Peppas, N. A. "Enzymatic biodegradation of hydrogels for protein delivery targeted to the small intestine", Biomacromolecules, 16(3), pp. 962–972, 2015. https://doi.org/10.1021/bm501871a

[41] Kulkarni, R. V., Sreedhar, V., Mutalik, S., Setty, C. M., Sa, B. "Interpenetrating network hydrogel membranes of sodium alginate and poly(vinyl alcohol) for prazosin hydrochloride through skin", International Journal of Biological Macromolecules, 47(4), pp. 520–527, 2010. https://doi.org/10.1016/j.ijbiomac.2010.07.009

[42] Samanta, H. S., Ray, S. K. "Controlled release of tinidazole and theophylline from chitosan based composite hydrogels", Carbohydrate Polymers, 106, pp. 109–120, 2014. https://doi.org/10.1016/j.carbpol.2014.01.097

[43] Bashir, S., Teo, Y. Y., Ramesh, S., Ramesh, K. "Synthesis, characterization, properties of N-succinyl chitosan-g-poly(methacrylic acid) hydrogels and *in vitro* release of theophylline", Polymer, 92, pp. 36–49, 2016. https://doi.org/10.1016/j.polymer.2016.03.045

[44] Donbrow, M., Samuelov, Y. "Zero order drug delivery from double-layered porous films: Release rate profiles from ethyl cellulose, hydroxypropyl cellulose and polyethylene glycol mixtures", Journal of Pharmacy and Pharmacology, 32(1), pp. 463–470, 1980. https://doi.org/10.1111/j.2042-7158.1980.tb12970.x

[45] Desai, S. J., Singh, P., Simonelli, A. P., Higuchi, W. I. "Investigation of factors influencing release of solid drug dispersed in inert matrices III.: Quantitative studies involving the polyethylene plastic matrix", Journal of Pharmaceutical Sciences, 55(11), pp. 1230–1234, 1966. https://doi.org/10.1002/jps.2600551113

[46] Korsmeyer, R. W., Gurny, R., Doelker, E., Buri, P., Peppas, N. A. "Mechanisms of solute release from porous hydrophilic polymers", International Journal of Pharmaceutics, 15(1), pp. 25–35, 1983. https://doi.org/10.1016/0378-5173(83)90064-9

[47] Babu, V. R., Hosamani, K. M., Aminabhavi, T. M. "Preparation and in-vitro release of chlorothiazide novel pH-sensitive chitosan-*N*,*N*′-dimethylacrylamide semi-interpenetrating network microspheres", Carbohydrate Polymers, 71(2), pp. 208–217, 2008. https://doi.org/10.1016/j.carbpol.2007.05.039